Accurate treatment of two-dimensional non-separable hindered internal rotors

Antonio Fernández-Ramos

Citation: J. Chem. Phys. **138**, 134112 (2013); doi: 10.1063/1.4798407
View online: http://dx.doi.org/10.1063/1.4798407
View Table of Contents: http://jcp.aip.org/resource/1/JCPSA6/v138/i13
Published by the American Institute of Physics.

Accurate treatment of two-dimensional non-separable hindered internal rotors

Antonio Fernández-Ramos[a)]
Department of Physical Chemistry and Center for Research in Biological Chemistry and Molecular Materials (CIQUS), Universidade de Santiago de Compostela, 15782 Santiago de Compostela, Spain

(Received 17 December 2012; accepted 13 March 2013; published online 4 April 2013)

This work presents an accurate way for calculating partition functions of strongly coupled hindered rotors in two dimensions. The two-dimensional torsional potential is generated from electronic structure calculations and fitted to Fourier series. The kinetic energy includes off-diagonal terms which are allowed to vary with the torsional angles, and these terms were also fitted to Fourier series. The resulting Hamiltonian leads to a coupled Schrödinger equation which was solved by the variational method. Therefore, the final two-dimensional non-separable (2D-NS) partition function incorporates coupling terms in both the kinetic and the potential energy. The methodology has been tested for propane, methyl formate, and a hydrogen abstraction transition state from propanone by the OH radical. How to incorporate the 2D-NS partition function in the total vibrational-rotational partition function is also discussed. © *2013 American Institute of Physics*. [http://dx.doi.org/10.1063/1.4798407]

I. INTRODUCTION

The calculation of thermal rate constants in reactions involving molecules with conformational flexibility is unavoidable linked to the problem of how to treat hindered internal rotations. This subject has gained importance in later years due to the increasing interest in the theoretical study of combustion reactions. Many of the molecules that participate in combustion (alkanes, alcohols, etc.) have many conformers with interconversions among them by torsional rotations about single chemical bonds. One way of treating these torsional motions is by the harmonic oscillator (HO) approximation, which is of very common use for the rest of the vibrational degrees of freedom. However, it has been long recognized, that the low rotational barriers for interconversion between conformers usually encountered, are a clear sign that anharmonicity plays an important role for these low-frequency torsional modes.[1,2]

Several one-dimensional models have been proposed and used in order to treat hindered internal torsions.[3–9] These methods can also deal with molecules with more than one torsion if these torsions are not coupled or weakly coupled, because in that case they can be separated.[10] However, there are systems in which torsions are coupled, both in the kinetic and potential energy terms, and it is more accurate to consider a non-separable approach. The path-integrals formalism can be used to take into account quantum effects and coupling in the potential energy.[11–17] It is also quite common to calculate the classical partition function[18] taking into account the global torsional potential.[19,20] In any case the calculation of a global torsional potential energy surface with the same dimensionality as the number of torsions is a very time consuming task.

Therefore a number of approximations have been designed in order to reduce the computational time while trying to retain the accuracy. For instance, Truhlar and co-workers have developed a series of multi-structural methods[21,22] that only require the location of the conformational minima of the torsional potential, and Van Speybroeck and co-workers[23,24] indicated that torsional coupling may be only important between neighboring torsions and that a high-dimensional torsional potential can be well approximated by a sum over two-dimensional potentials. This is an interesting approach because it is well-known that two-dimensional potentials can be accurately fitted by Fourier-type series as have been shown by Durig and co-workers[25,26] and others.[27] Those analytical potentials can be used to calculate two-dimensional classical partition functions[28] to which it is easy to add quantum corrections.[29] One way to do that is to use the approximation by Pitzer and Gwinn,[2] in which the quantum effects are calculated as the ratio between the quantum and classical HO partition functions corresponding to the torsional modes. However, this approximation may introduce substantial error if the torsional modes are coupled. This is the starting point of this treatment that leads to the quantum two-dimensional non-separable (2D-NS) partition function. Specifically, I propose a two-dimensional quantum method that goes beyond that approximation, and that incorporates coupling terms in both the potential and kinetic energy. The latter through the method developed by Kilpatrick and Pitzer.[30] The 2D-NS partition function is calculated for propane, **S1,** methyl formate (also called methyl methanoate), **S2**, and the transition state structures of the hydrogen abstraction reaction of propanone by the OH radical, system **S3**.

For these three systems, the two-dimensional torsional potentials and the kinetic energy terms of the dihedrals shown in Fig. 1 are calculated and fitted to Fourier series. With these analytical Hamiltonian, it is possible to solve the Schrödinger equation by the variational method and to calculate the 2D-NS partition function (as shown in Sec. II). Section II also describes a convenient way to incorporate the two-dimensional partition function into the total vibrational-rotational (or

a)Electronic mail: qf.ramos@usc.es

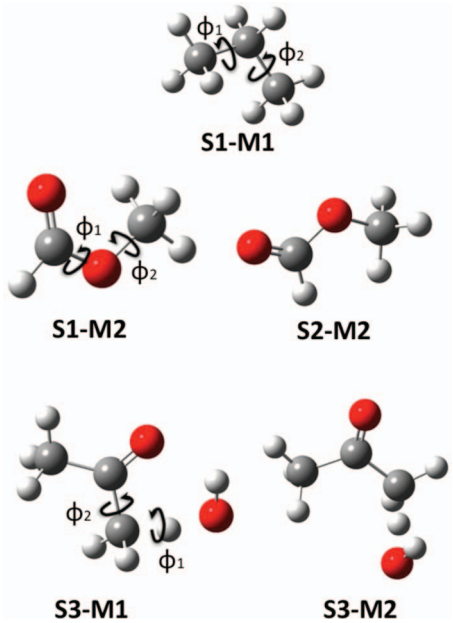

FIG. 1. Balls and sticks models representing the stationary points and the two torsional angles for systems **S1**, **S2**, and **S3**. It also indicates the two torsional angles studied in each case. For **S3** the hindered rotation ϕ_1 is about the C, O atoms.

rovibrational) partition function. Section III discusses the results obtained with this new method and compares them with some previous models.

II. METHODOLOGY

A. The two-dimensional non-separable torsional partition function

The seminal work of Kilpatrick and Pitzer[30] showed that the kinetic energy of a molecule presenting several rotating tops is given by

$$T_{\text{rot-tor}} = \frac{1}{2}\boldsymbol{\omega}^{\dagger}_{\text{rot-tor}}\mathbf{S}\boldsymbol{\omega}_{\text{rot-tor}}, \tag{1}$$

where $\boldsymbol{\omega}^{\dagger}_{\text{rot-tor}}$ and $\boldsymbol{\omega}_{\text{rot-tor}}$ are the row and column vectors of angular velocities and **S** is a square matrix of length $3 + t$ that includes the rotation of the whole molecule and the torsions (being t the number of torsions). The **S** matrix by means of a congruent transformation gives a diagonal matrix with the principal moments of inertia of the overall rotation plus a reduced **D** matrix with the coupled torsions. The rotation of the molecule can now be separated from the torsional motions and the kinetic energy of Eq. (1) can be rewritten as

$$T_{\text{rot-tor}} = \frac{1}{2}\boldsymbol{\omega}^{\dagger}_{\text{rot}}\mathbf{I}\boldsymbol{\omega}_{\text{rot}} + \frac{1}{2}\boldsymbol{\omega}^{\dagger}_{\text{tor}}\mathbf{D}\boldsymbol{\omega}_{\text{tor}}. \tag{2}$$

The first term of the right-side of Eq. (2) represents the kinetic energy of the overall rotation, being **I** the diagonal matrix containing the principal moments of inertia of the molecule, whereas the second term of the right-side of Eq. (2) deals with the torsions. It should be noticed that the **S** matrix is affected by the torsional motion, and therefore both the principal moments of inertia of the molecule and the **D** matrix are also affected by the torsional motion. Pitzer[31] argued that a good approximation would be to calculate the **S** matrix only at the equilibrium geometry because the change in the product of the moments of inertia with the torsional angles roughly compensates the change in the product of vibrational frequencies, so the final rovibrational partition function remains unaltered. In this work some of the dependence of the overall rotation and molecular vibrations with the torsional angles is included (as discussed in Subsection II C), whereas the dependence of the **D** matrix with the torsional angles is fully taken into account. Therefore the torsional part of the kinetic energy for two coupled (non-separable) torsions ϕ_1 and ϕ_2 written in matrix form is given by[2,31]

$$\begin{aligned} 2T_{\text{tor}} &= \dot{\boldsymbol{\phi}}^{\dagger}\mathbf{D}(\phi_1,\phi_2)\dot{\boldsymbol{\phi}} \\ &= (\dot{\phi}_1,\dot{\phi}_2)\begin{pmatrix} I_1(\phi_1,\phi_2) & -\Lambda_{1,2}(\phi_1,\phi_2) \\ -\Lambda_{1,2}(\phi_1,\phi_2) & I_2(\phi_1,\phi_2)\end{pmatrix}\begin{pmatrix}\dot{\phi}_1\\ \dot{\phi}_2\end{pmatrix}, \end{aligned} \tag{3}$$

where $\dot{\phi}_\tau = \frac{d\phi_\tau}{dt}$, with $\tau = 1, 2$. In general the $\mathbf{D}(\phi_1,\phi_2)$ matrix is non-diagonal, and the two elements along the diagonal, i.e., $I_1(\phi_1, \phi_2)$ and $I_2(\phi_1, \phi_2)$, correspond to the reduced moments of inertia calculated using the relations given by Pitzer,[31] which are exact for molecules with one or more uncoupled internal rotors [$I^{(3,4)}$ in the notation of East and Radom[29]]. The off-diagonal term $-\Lambda_{12}(\phi_1, \phi_2)$ accounts for the coupling between the two reduced moments of inertia, and in this work that coupling was calculated by using the exact treatment described by Kilpatrick and Pitzer (see Ref. 30 for details).

Equation (3) can be written in terms of the angular momentum of the rotors. Taking into account that

$$L_\tau = \frac{\partial T_{\text{tor}}}{\partial \dot{\phi}_\tau}, \tag{4}$$

the following expression is obtained:

$$\boldsymbol{L} = \mathbf{D}(\phi_1,\phi_2)\dot{\boldsymbol{\phi}}. \tag{5}$$

The substitution of Eq. (5) into Eq. (3) leads to

$$\begin{aligned} 2T_{\text{tor}} &= \{[\mathbf{D}(\phi_1,\phi_2)]^{-1}\boldsymbol{L}\}^{\dagger}\mathbf{D}(\phi_1,\phi_2)[\mathbf{D}(\phi_1,\phi_2)]^{-1}\boldsymbol{L} \\ &= \boldsymbol{L}^{\dagger}[\mathbf{D}(\phi_1,\phi_2)]^{-1}\boldsymbol{L}, \end{aligned} \tag{6}$$

where $[\mathbf{D}(\phi_1,\phi_2)]^{-1}$ is the inverse of the $\mathbf{D}(\phi_1,\phi_2)$ matrix, i.e.,

$$\begin{aligned} [\mathbf{D}(\phi_1,\phi_2)]^{-1} &= \frac{1}{|\mathbf{D}(\phi_1,\phi_2)|}\begin{pmatrix} I_2(\phi_1,\phi_2) & \Lambda_{1,2}(\phi_1,\phi_2) \\ \Lambda_{1,2}(\phi_1,\phi_2) & I_1(\phi_1,\phi_2)\end{pmatrix} \\ &= \begin{pmatrix} d_{11} & d_{12} \\ d_{12} & d_{22}\end{pmatrix} \end{aligned} \tag{7}$$

and $|\mathbf{D}(\phi_1,\phi_2)| = \mathrm{I}_1\mathrm{I}_2 - \Lambda_{12}^2$ is the determinant of the $\mathbf{D}(\phi_1,\phi_2)$ matrix.

Turning now to quantum mechanics by replacing the classical angular momentum by $L_\tau = -i\hbar\frac{\partial}{\partial\phi_\tau}$, the kinetic energy operator due to the two-dimensional torsional motion is given by

$$T_{\text{tor}}\left(\frac{\partial}{\partial\phi_1},\frac{\partial}{\partial\phi_2}\right) = -\frac{\hbar}{2}\sum_{\tau=1}^{2}\sum_{\varsigma=1}^{2} d_{\tau\varsigma}\frac{\partial^2}{\partial\phi_\tau\partial\phi_\varsigma} + \frac{\partial d_{\tau\varsigma}}{\partial\phi_\tau}\frac{\partial}{\partial\phi_\varsigma}, \tag{8}$$

where the elements $d_{\tau\varsigma}$, $\tau = 1, 2$; $\varsigma = 1, 2$ are those of the inverse matrix of Eq. (7).

The Hamiltonian for two strongly coupled (non-separable) torsions ϕ_1 and ϕ_2 can be written as

$$H_{\text{tor}}\left(\frac{\partial}{\partial\phi_1}, \frac{\partial}{\partial\phi_2}; \phi_1, \phi_2\right) = T_{\text{tor}}\left(\frac{\partial}{\partial\phi_1}, \frac{\partial}{\partial\phi_2}\right) + V_{\text{tor}}(\phi_1, \phi_2), \tag{9}$$

where the kinetic energy is given by Eq. (8), and the two-dimensional potential is written in the form

$$V_{\text{tor}}(\phi_1, \phi_2) = V_1(\phi_1) + V_2(\phi_2) + V^{2\text{D}}(\phi_1, \phi_2). \tag{10}$$

The two torsions are separable if $V^{2\text{D}}(\phi_1, \phi_2)$, the coupling term $-\Lambda_{12}$, and the dependence of the reduced moments of inertia with the torsional angles are negligible. In this case the problem is reduced to two independent one-dimensional hindered rotors given by the following Hamiltonian:

$$H_\tau = \frac{-\hbar^2}{2}\left\{\frac{1}{I_\tau}\frac{d^2}{d\phi_\tau^2}\right\} + V_\tau^{1\text{D}}(\phi_\tau), \quad \tau = 1, 2. \tag{11}$$

It is possible to solve Eq. (11) by representing the torsional potentials $V_1^{1\text{D}}$ and $V_2^{1\text{D}}$ by Fourier series of the type

$$V_1^{1\text{D}}(\phi_1) = a_0 + \sum_{M=1}^{M_{\max}} a_M \cos(M\phi_1) + \sum_{M'=1}^{M'_{\max}} a'_{M'} \sin(M'\phi_1) \tag{12}$$

and

$$V_2^{1\text{D}}(\phi_2) = b_0 + \sum_{N=1}^{N_{\max}} b_N \cos(N\phi_2) + \sum_{N'=1}^{N'_{\max}} b'_{N'} \sin(N'\phi_2), \tag{13}$$

where $a_0, b_0, a_M\,(M = 1, \ldots, M_{\max}), a'_{M'}\,(M' = 1, \ldots, M'_{\max})$, $b_N\,(N = 1, \ldots, N_{\max})$, and $b'_{N'}\,(N' = 1, \ldots, N'_{\max})$ are fitting parameters. The trial wavefunctions will be linear combinations of the wavefunctions which are solution for the Schrödinger equation of the particle in a ring, i.e.,

$$\Phi_1(\phi_1) = \frac{1}{\sqrt{2\pi}} \sum_{k=-k_{\max}}^{k_{\max}} c_{1,k} e^{ik\phi_1} \tag{14}$$

and

$$\Phi_2(\phi_2) = \frac{1}{\sqrt{2\pi}} \sum_{n=-n_{\max}}^{n_{\max}} c_{2,n} e^{in\phi_2}. \tag{15}$$

A typical value for the integers $k_{\max}$ and $n_{\max}$ that produces convergent results is 100. The matrix elements of Hamiltonians H_1 and H_2 using the potentials of Eqs. (12) and (13), and trial functions from Eqs. (14) and (15) are

$$\langle j|H_1|k\rangle = \frac{\hbar^2 k^2}{2I_1}\delta_{jk} + \langle j|V_1^{1\text{D}}|k\rangle, \tag{16}$$

where

$$\langle j|V_1^{1\text{D}}|k\rangle = a_0\delta_{jk} + \frac{a_M}{2}\delta_{|j-k|M} - i\frac{a_{M'}}{2}\text{sgn}(j-k)\delta_{|j-k|M'}, \tag{17}$$

and

$$\langle m|H_2|n\rangle = \frac{\hbar^2 n^2}{2I_2}\delta_{mn} + \langle m|V_2^{1\text{D}}|n\rangle, \tag{18}$$

where

$$\langle m|V_2^{1\text{D}}|n\rangle = b_0\delta_{mn} + \frac{b_N}{2}\delta_{|m-n|N} - i\frac{b_{N'}}{2}\text{sgn}(m-n)\delta_{|m-n|N'}, \tag{19}$$

respectively, being δ the delta of Kronecker, and sgn(x) the sign function. Details about the solution of the integrals is given in the supplementary material.[32] The diagonalization of each of the two secular matrices obtained from Eqs. (16) and (18) allows the calculation of the partition function by direct summation of the eigenvalues. Ellingson *et al.*[7] used the above method to obtain accurate one-dimensional hindered rotor partition functions, and they refer to that method as torsional eigenvalue summation (TES). Those authors only included cosine functions in the Fourier series. It fits well potentials with symmetry because the cosine is an even function; however sine functions are needed to fit asymmetric potentials.[33] This is probably the best one can do to treat multidimensional hindered rotors that are independent, because in this case the problem is reduced to a product of one-dimensional hindered rotor partition functions.

Therefore, the partition function for the two separable (S) torsions τ obtained by the TES method is given by

$$Q_{\text{tor}}^{\text{STES}} = q_1^{\text{TES}} q_2^{\text{TES}} \tag{20}$$

with

$$q_\tau^{\text{TES}} = \frac{1}{\sigma_\tau}\sum_j e^{-\beta\varepsilon_{\tau,j}}, \quad \tau = 1, 2 \tag{21}$$

being $\beta = 1/k_BT$, k_B is the Boltzmann constant, and T is the temperature; $\varepsilon_{1,j}$ and $\varepsilon_{2,j}$ are the eigenvalues (energies) after diagonalization of the secular matrices with the matrix elements obtained from Eqs. (16) and (18). The symmetry number of the internal rotation τ is given by σ_τ.

If the two torsions are not separable, a good fitting to the potential by Fourier series needs cross terms. In this case the potential can be written as

$$\begin{aligned} V_{\text{tor}}(\phi_1, \phi_2) = {} & V_1(\phi_1) + V_2(\phi_2) \\ & + \sum_{L_1=1}^{L_{1,\max}}\sum_{L_2=1}^{L_{2,\max}} c_{L_1L_2}\cos(L_1\phi_1)\cos(L_2\phi_2) \\ & + \sum_{P_1=1}^{P_{1,\max}}\sum_{P_2=1}^{P_{2,\max}} d_{P_1P_2}\sin(P_1\phi_1)\sin(P_2\phi_2) \\ & + \sum_{L'_1=1}^{L'_{1,\max}}\sum_{L'_2=1}^{L'_{2,\max}} c'_{L'_1L'_2}\cos(L'_1\phi_1)\sin(L'_2\phi_2) \\ & + \sum_{P'_1=1}^{P'_{1,\max}}\sum_{P'_2=1}^{P'_{2,\max}} d'_{P'_1P'_2}\sin(P'_1\phi_1)\cos(P'_2\phi_2), \end{aligned} \tag{22}$$

where $c_{L_1L_2}$, $L_1 = 1, \ldots, L_{1,\max}$, $L_2 = 1, \ldots, L_{2,\max}$, $d_{P_1P_2}$, $P_1 = 1, \ldots, P_{1,\max}$, $P_2 = 1, \ldots, P_{2,\max}$, $c'_{L'_1L'_2}$, $L'_1 = 1, \ldots, L'_{1,\max}$, $L'_2 = 1, \ldots, L'_{2,\max}$, and $d'_{P'_1P'_2}$, $P'_1 = 1, \ldots, P'_{1,\max}$, $P'_2 = 1, \ldots, P'_{2,\max}$ are fitting parameters, and $L_{1,\max}$, $L_{2,\max}$, $L'_{1,\max}$, $L'_{2,\max}$, $P_{1,\max}$, $P_{2,\max}$, $P'_{1,\max}$, and $P'_{2,\max}$ indicate the largest number of each series.

Once the number of terms for each of the series of Eq. (22) are known, the same type of series are used to fit each of the elements of the inverse of the $\mathbf{D}(\phi_1, \phi_2)$ matrix of Eq. (7), i.e.,

$$\begin{aligned} d_{\tau\varsigma} = {} & F_1^{\tau,\varsigma}(\phi_1) + F_2^{\tau,\varsigma}(\phi_2) \\ & + \sum_{L_1=1}^{L_{1,\max}} \sum_{L_2=1}^{L_{2,\max}} c_{L_1L_2}^{\tau,\varsigma} \cos(L_1\phi_1)\cos(L_2\phi_2) \\ & + \sum_{P_1=1}^{P_{1,\max}} \sum_{P_2=1}^{P_{2,\max}} d_{P_1P_2}^{\tau,\varsigma} \sin(P_1\phi_1)\sin(P_2\phi_2) \\ & + \sum_{L_1'=1}^{L_{1,\max}'} \sum_{L_2'=1}^{L_{2,\max}'} c_{L_1'L_2'}^{\prime\tau,\varsigma} \cos(L_1'\phi_1)\sin(L_2'\phi_2) \\ & + \sum_{P_1'=1}^{P_{1,\max}'} \sum_{P_2'=1}^{P_{2,\max}'} d_{P_1'P_2'}{}'\tau,\varsigma \sin(P_1'\phi_1)\cos(P_2'\phi_2). \end{aligned} \quad (23)$$

The one-dimensional terms of Eq. (23) are similar to Eqs. (12) and (13) and given by

$$F_1^{\tau,\varsigma}(\phi_1) = a_0^{\tau\varsigma} + \sum_{M=1}^{M_{\max}} a_M^{\tau\varsigma} \cos(M\phi_1) + \sum_{M'=1}^{M'_{\max}} a_{M'}^{\prime\tau\varsigma} \sin(M'\phi_1) \quad (24)$$

and

$$F_2^{\tau,\varsigma}(\phi_2) = b_0^{\tau\varsigma} + \sum_{N=1}^{N_{\max}} b_N^{\tau\varsigma} \cos(N\phi_2) + \sum_{N'=1}^{N'_{\max}} b_N^{\prime\tau\varsigma} \sin(N'\phi_2). \quad (25)$$

The substitution of the terms of Eq. (23) and of the potential of Eq. (22) into Eq. (9) using the trial wavefunction $\Phi(\phi_1, \phi_2) = \Phi_1(\phi_1)\Phi_2(\phi_2)$, leads to matrix elements of the Hamiltonian given by

$$\begin{aligned} \langle jm|H|kn\rangle = {} & \frac{\hbar}{2}\{n^2\langle jm|d_{11}|kn\rangle + 2nk\langle jm|d_{12}|kn\rangle \\ & + k^2\langle jm|d_{22}|kn\rangle\} \\ & - \frac{\hbar}{2}\langle jm| \sum_{\tau=1}^{2}\sum_{\varsigma=1}^{2} \frac{\partial d_{\tau\varsigma}}{\partial\phi_\tau}\frac{\partial}{\partial\phi_\varsigma}|kn\rangle \\ & + \langle j|V_1|k\rangle\delta_{mn} + \langle m|V_2|n\rangle\delta_{jk} + \langle jm|V_{12}|kn\rangle, \end{aligned} \quad (26)$$

where

$$\begin{aligned} \langle jm|V_{12}|kn\rangle = {} & \frac{1}{4}\{c_{L_1L_2}\delta_{|j-k|L_1}\delta_{|m-n|L_2} - d_{P_1P_2}\mathrm{sgn}(j-k) \\ & \times \mathrm{sgn}(m-n)\delta_{|j-k|P_1}\delta_{|m-n|P_2}\} \\ & - \frac{i}{4}\{c'_{L_1'L_2'}\mathrm{sgn}(m-n)\delta_{|j-k|L_1'}\delta_{|m-n|L_2'} \\ & + d'_{P_1'P_2'}\mathrm{sgn}(j-k)\delta_{|j-k|P_1'}\delta_{|m-n|P_2'}\}. \end{aligned} \quad (27)$$

The $\langle jm|d_{\tau\varsigma}|kn\rangle$ terms of the kinetic energy are a sum of kinetic energy contributions with the same expression as Eq. (27) of the potential but with the coefficients of Eq. (23). The terms depending on the derivative of $d_{\tau\varsigma}$ in Eq. (27) are given in the supplementary material.[32]

Similar potentials to the one of Eq. (22) have been used often in the past to calculate accurate torsional frequencies and the transitions between them.[25–27,34–36] However, our objective is to obtain a large number of eigenvalues to be able to calculate converged quantum partition functions till temperatures at which the classical partition function takes over.

Two important things should be mentioned at this stage: (1) The trial wavefunction includes a double sum which leads to squared matrix of length $(2k_{\max} + 1) \times (2n_{\max} + 1)$. If $k_{\max} = n_{\max} = 100$ to obtain the eigenvalues by full diagonalization is cumbersome. However, most of the matrix elements are zero, so it is possible to use properties of the sparse matrices to calculate a large number of eigenvalues. The quantum partition function obtained from the direct sum of the eigenvalues is called 2D-NS and given by

$$Q_{\mathrm{tor}}^{\mathrm{2D-NS}} = \frac{1}{\sigma_{\mathrm{tor}}}\sum_j e^{-\beta E_{\mathrm{tor},j}}, \quad (28)$$

where

$$\sigma_{\mathrm{tor}} = \sigma_1\sigma_2 \quad (29)$$

being σ_1 and σ_2 the symmetry numbers associated to the internal rotation about ϕ_1 and ϕ_2, respectively, and $E_{\mathrm{tor},j}$ the eigenvalues. (2) The classical equivalent to the partition function of Eq. (28) is

$$Q_{\mathrm{cl,tor}} = \frac{1}{\sigma_{\mathrm{tor}}}\frac{1}{2\pi\beta\hbar^2}\int_0^{2\pi}\int_0^{2\pi} d\phi_1 d\phi_2 |\mathbf{D}(\phi_1,\phi_2)|^{1/2} \mathrm{e}^{-\beta \mathrm{V}(\phi_1,\phi_2)}, \quad (30)$$

and, therefore Eqs. (28) and (30) should coincide at high temperatures.

B. 2D-NS vs Pitzer and Gwinn

It is interesting to compare Eq. (28) with the torsional partition function proposed by Pitzer and Gwinn[2] (TPG). The TPG partition function is given by

$$Q_{\mathrm{tor}}^{\mathrm{TPG}} = \frac{\overline{Q}_{\mathrm{tor}}^{\mathrm{HO}}}{\overline{Q}_{\mathrm{tor}}^{\mathrm{CHO}}} Q_{\mathrm{cl,tor}}, \quad (31)$$

where $Q_{\mathrm{cl,\,tor}}$ is given by Eq. (30). In the original derivation the $\mathbf{D}$ matrix was evaluated only at the absolute minimum of the torsional potential, but here the variation with the torsional angles is allowed. The TPG partition function reaches the correct high temperature limit and it accounts for the quantum effects within the HO approximation, i.e., by considering the ratio between the quantum HO partition function given by

$$\overline{Q}_{\mathrm{tor}}^{\mathrm{HO}} = \prod_{\tau=1}^{t} \overline{q}_\tau^{\mathrm{HO}} \quad (32)$$

being

$$\overline{q}_\tau^{\mathrm{HO}} = \frac{e^{-\beta\hbar\overline{\omega}_\tau/2}}{1 - e^{-\beta\hbar\overline{\omega}_\tau}}, \quad (33)$$

and the classical HO partition function

$$\overline{Q}_{\rm tor}^{\rm CHO} = \prod_{\tau=1}^{t} \frac{1}{\beta\hbar\overline{\omega}_\tau}. \tag{34}$$

In this case the products in both Eqs. (32) and (34) run over $t = 2$ torsional frequencies, and the frequencies $\overline{\omega}_\tau$ are not normal mode frequencies, but those associated with the absolute minimum of two-dimensional torsional potential. An approximated way of calculating these frequencies is

$$\overline{\omega}_\tau^\star = \sqrt{\frac{1}{I_\tau}\left(\frac{\partial^2 V}{\partial\phi_\tau^2}\right)_{\phi_\tau=\phi_{\tau,e}}}, \quad \tau = 1, 2 \tag{35}$$

being I_τ the reduced moment of inertia and $\phi_{\tau,e}$ the value of the torsional angle ϕ_τ at the minimum. A more rigorous way to calculate the HO torsional frequencies is to consider also the cross terms in both the reduced moments of inertia and the force constants. The latter given by the second derivative of the torsional potential. The new frequencies can be calculated from the the eigenvalues of the secular determinant involving the **D** matrix and the torsional force constants matrix,[31] i.e.,

$$|\mathbf{K} - \overline{\omega}_\tau \mathbf{D}| = 0 \tag{36}$$

being

$$\mathbf{K} = \begin{pmatrix} \frac{\partial^2 V}{\partial\phi_1^2} & \frac{\partial^2 V}{\partial\phi_1\partial\phi_2} \\ \frac{\partial^2 V}{\partial\phi_1\partial\phi_2} & \frac{\partial^2 V}{\partial\phi_2^2} \end{pmatrix}. \tag{37}$$

However, the classical partition function is built from all the conformers that can be reached by the t-dimensional hindered rotor potential (in this case $t = 2$), not just the lowest minimum, and the rest of coordinates are minimized at every point along this potential. Thus, the landscape of the potential presents a number of minima, being the number of conformers, n_C (distinguishable configurations), the total number of minima of the torsional potential divided by the symmetry number of Eq. (29).[37] In this context, provided that the quantum effects are well represented by the HO approximation, it seems more adequate to substitute the TPG partition function by a new multi-conformational TPG partition function (MC-TPG), which is given by

$$Q_{\rm tor}^{\rm MC-TPG} = \frac{\overline{Q}_{\rm tor}^{\rm MC-HO}}{\overline{Q}_{\rm tor}^{\rm MC-CHO}} Q_{\rm cl,tor}, \tag{38}$$

where the multi-conformer torsional HO partition function is

$$\overline{Q}_{\rm tor}^{\rm MC-HO} = \sum_{i=1}^{n_{\rm C}} e^{-\beta U_i} \prod_{\tau=1}^{t} \overline{q}_{i,\tau}^{\rm HO} \tag{39}$$

and the multi-conformer classical HO partition function would be given by

$$\overline{Q}_{\rm tor}^{\rm MC-CHO} = \sum_{i=1}^{n_{\rm C}} e^{-\beta U_i} \prod_{\tau=1}^{t} \frac{1}{\beta\hbar\overline{\omega}_{i,\tau}}. \tag{40}$$

The frequency $\overline{\omega}_{i,\tau}$ is associated to torsion τ at the ith minimum of the potential and given by Eq. (36).

Using the above relations, the MC-TPG partition function of Eq. (38) is given by

$$Q_{\rm tor}^{\rm MC-TPG} = F^{\rm MC-PG} F_{\rm c} \overline{Q}_{\rm tor}^{\rm MC-CHO} \tag{41}$$

being

$$F^{\rm MC-PG} = \frac{\overline{Q}_{\rm tor}^{\rm MC-HO}}{\overline{Q}_{\rm tor}^{\rm MC-CHO}} \tag{42}$$

and

$$F_{\rm c} = \frac{Q_{\rm cl,tor}}{\overline{Q}_{\rm tor}^{\rm MC-CHO}}. \tag{43}$$

The term $F_{\rm c}$ takes into account the couplings in both the kinetic an potential energies.

Similarly, the two-dimensional partition function of Eq. (28) can be written as

$$Q_{\rm tor}^{\rm 2D-NS} = F_{\rm q} F_{\rm c} \overline{Q}_{\rm tor}^{\rm MC-CHO}, \tag{44}$$

where

$$F_{\rm q} = \frac{Q_{\rm tor}^{\rm 2D-NS}}{Q_{\rm cl,tor}}. \tag{45}$$

The deviations of MC-TPG from the 2D-NS partition function are collected in the ratio

$$\frac{Q_{\rm tor}^{\rm 2D-NS}}{Q_{\rm tor}^{\rm MC-TPG}} = \frac{F_{\rm q}}{F^{\rm MC-PG}}. \tag{46}$$

This relation can be seen as a deviation from the HO treatment of quantum effects. In the case of TES, the ratio $Q_{\rm tor}^{\rm 2D-NS}/Q_{\rm tor}^{\rm STES}$ is associated to the influence of coupling in the quantum effects.

C. The multi-conformational rovibrational partition function

Although this work deals with the evaluation of two-dimensional hindered rotor partition functions, below I describe an easy way of incorporating this partition function into the total rovibrational partition function. The latter can be built accurately by taking into account rotational-vibrational coupling.[38] It has to include corrections due to the variations of geometry by the rotation about the torsional angles, since these changes have effect on the principal axes of inertia and in the vibrations of the system. However, to calculate Hessians for several dispositions of the torsional angles can be very expensive in computer time, so it is interesting to work in the line of Eqs. (39) and (40).[21,37,39] These two equations take the geometric effects partially into account by expressing the total harmonic rovibrational partition function, $\tilde{Q}_{\rm har}$, for a number of conformers $n_{\rm C}$, as a sum of the rovibrational partition functions of the individual conformers

$$\tilde{Q}_{\rm har} = \sum_{i=1}^{n_{\rm C}} Q_i^{\rm RRHO}. \tag{47}$$

The tilde over the Q letter is used to indicate that this is the total multi-conformational rovibrational partition function. The

superscript RRHO indicates that the rigid-rotor (RR) HO approximation is invoked. Therefore, for each conformer

$$Q_i^{\mathrm{RRHO}} = Q_{\mathrm{rot},i}\, Q_i^{\mathrm{HO}} e^{-\beta U_i} \tag{48}$$

is the product of the classical rigid-rotor rotational partition function $Q_{\mathrm{rot},i}$, the Q_i^{HO} normal-mode harmonic oscillator quantum vibrational partition function, and the Boltzmann factor that includes the difference in energy U_i with respect to the most stable conformer. It should be noticed that each of the rotational partition functions should include the symmetry number for external rotation of the whole molecule.[37]

To introduce the two-dimensional partition function of Eq. (28), the HO oscillator frequencies due to the two torsions have to be removed from the total rovibrational partition function of Eq. (47). There are several approximated ways of doing that, for instance one can directly remove the normal-mode frequencies mainly associated to the torsions. Other option is to define non-redundant internal coordinates to identify the force constants corresponding to the torsions. At this point, the torsional frequencies can be obtained using Eq. (35), as indicated in Ref. 21. The former procedure is quite approximate if the normal mode is not a pure torsion, whereas the latter does not include the coupling between the torsions. Here, I propose to use the HO torsional frequencies obtained from Eq. (36). Those include the coupling between the torsions, and in the line of Eq. (47), if we take into account all the distinguishable wells of the torsional potential, the torsional multi-former HO partition function of Eq. (39) is obtained.

Therefore, the total multidimensional partition function $\tilde{Q}_{\mathrm{tor}}^{\mathrm{MD}}$ including the anharmonic treatment for torsions described in this work is expressed as

$$\tilde{Q}_{\mathrm{tor}}^{\mathrm{MD}} = Q_{\mathrm{tor}}^{\mathrm{2D-NS}} \frac{\tilde{Q}_{\mathrm{har}}}{\overline{Q}_{\mathrm{tor}}^{\mathrm{MC-HO}}} \tag{49}$$

or

$$\tilde{Q}_{\mathrm{tor}}^{\mathrm{MD}} = \alpha_{\mathrm{tor}}^{\mathrm{2D-NS}} \tilde{Q}_{\mathrm{har}}, \tag{50}$$

being

$$\alpha_{\mathrm{tor}}^{\mathrm{2D-NS}} = \frac{Q_{\mathrm{tor}}^{\mathrm{2D-NS}}}{\overline{Q}_{\mathrm{tor}}^{\mathrm{MC-HO}}}. \tag{51}$$

The parameter $\alpha_{\mathrm{tor}}^{\mathrm{2D-NS}}$ enters as multiplicative coefficient that includes deviations from the harmonic multi-conformer partition function, when torsions are calculated with the 2D-NS anharmonic treatment, instead of with the harmonic approximation.

D. Computational details

All the electronic structure calculations were performed at the MPWB1K method,[40] with the augmented polarized double-ζ basis set, 6-31+G(d,p).[41] This level is not very expensive in computer time and has shown to perform well for nonmetallic thermochemical data and thermochemistry.[42] The energies, geometries, and normal-mode frequencies of all the stationary points depicted in Fig. 1 are listed in the supplementary material.[32] The two-dimensional torsional potential energy surfaces for each of the systems were generated by optimizing all the degrees of freedom, but the two torsions, using a stepsize of 10° (usually, converged results are obtained with a stepsize of 15°, but for quite asymmetric torsional potentials as for system **S3** a stepsize of 10° is needed). The elements of the **D** matrix were evaluated at each of the geometries as described in Ref. 30 and implemented in Ref. 43. The frequencies calculated at each of the stationary points were scaled by 0.964.[44]

The potential energy grid obtained from the electronic structure calculations was fitted to Fourier series. In the fitting procedure it is possible to use reference one-dimensional potentials, i.e., potentials in which one of the dihedrals is kept constant at a given reference value

$$V_1^{\mathrm{ref}}(\phi_1) = V_{\mathrm{tor}}\left(\phi_1, \phi_2^{\mathrm{ref}}\right), \quad V_2^{\mathrm{ref}}(\phi_2) = V_{\mathrm{tor}}\left(\phi_1^{\mathrm{ref}}, \phi_2\right). \tag{52}$$

The obvious choice is to use the torsional angles of the absolute minimum as reference. However, that reference leads to a very unsatisfactory fitting; it is better to perform an unrestricted fit using Fourier series, and searching, *a posteriori*, for ϕ_1^{ref} and ϕ_2^{ref}. The resulting one-dimensional potentials of Eq. (10) can be approximately identified to reference potentials with $\phi_1^{\mathrm{ref}} = \phi_2^{\mathrm{ref}} = 99°$ for propane, $\phi_1^{\mathrm{ref}} = 9°$ and $\phi_2^{\mathrm{ref}} = 180°$ for methyl formate, and $\phi_1^{\mathrm{ref}} = 68°$ and $\phi_2^{\mathrm{ref}} = 284°$ for system **S3**.

A second finer grid with stepsize every 1° was generated from the electronic structure calculations. The extra points on this second grid were obtained by fitting the data to a two-dimensional spline under tension.[45] To guarantee that the Fourier series accurately represent the potential, it was required that both grids (the one fitted to Fourier series and the one fitted to the spline) would lead to classical partition functions, calculated by Eq. (22), differing by less than 0.5% in all the temperature range between $T = 100$ and 2000 K. The classical partition functions were evaluated by numerical integration using the trapezoidal rule with a stepsize of 1°. In this iterative procedure, the elements of the **D** matrix introduced in the two classical partition functions were always those obtained by fits to splines under tension. Once the fit of the potential to the Fourier series is satisfactory, I proceed to fit the elements of the **D** matrix to Fourier series. These are very well reproduced by assuming the same number of terms as for the potential. All the fits to Fourier series were carried out by the GNUplot program.[46]

The calculation of the eigenvectors was carried out with the help of JADAMILU software.[47] In particular, the eigenvalues from the matrix elements of Eq. (26) were obtained by several runs of JADAMILU, which allows the calculation of a selected number of eigenvalues in very large real or complex symmetric Hermitian sparse matrices. The calculation of $Q_{\mathrm{tor}}^{\mathrm{2D-NS}}$ was carried out by the HR2D program.[48]

In the case of propane, the torsional potential was taken from Durig *et al.*[34] Those authors obtained the potential by fitting spectroscopic data to Fourier series. The geometry of the minimum to calculate the reduced moments of inertia and the harmonic frequencies was obtained at the MPWB1K/6-31+G(d,p) level, as for the other two systems.

TABLE I. Parameters (in cm^{-1}) for the one-dimensional terms of Eq. (22) for the three systems.

Parameter	S1	S2	S3
$a_0 + b_0$	1235.1	3114.4	818.4
a_1, a'_1	...	−831.4, ...	−94.6, 196.0
a_2, a'_2	...	−2074.7, ...	−42.3, 106.3
a_3, a'_3	−661.7, ...	−120.6, ...	−10.7, 32.4
a_4, a'_4	...	74.1, ...	−1.20, 16.2
a_5, a'_5	...	8.36, ...	1,76, 2.86
a_6, a'_6	...	−6.03, ...	0.80, 1.36
a_9, a'_9	...	...	0.34, 1.15
b_1, b'_1	...	...	269.2, ...
b_2, b'_2	...	...	322.0, ...
b_3, b'_3	−661.7, ...	139.5, ...	−84.7, ...
b_4, b'_4	...	...	22.4, ...
b_5, b'_5	...	...	−6.40, ...
b_6, b'_6	...	...	11.5, ...
b_7, b'_7	...	...	5.56, ...
b_8, b'_8	...	...	6.22, ...
b_9, b'_9	...	...	4.20, ...

TABLE II. Coupling parameters (in cm^{-1}) of Eq. (22) for the three systems.

Parameter	S1	S2	S3
c_{11}, d_{11}	...	...	−523.8, ...
c_{12}, d_{12}	...	...	−134.5, ...
c_{13}, d_{13}	...	15.9, 38.9	−17.0, ...
c_{14}, d_{14}	...	...	−5.00, ...
c_{21}, d_{21}	...	...	−175.0, ...
c_{22}, d_{22}	...	...	−100.0, ...
c_{23}, d_{23}	...	−112.1, −129.3	−27.1, ...
c_{24}, d_{24}	...	...	−22.6, ...
c_{31}, d_{31}	...	...	−44.1, ...
c_{32}, d_{32}	...	...	−45.0, ...
c_{33}, d_{33}	88.3, −66.0	71.4, 59.9	−27.0, ...
c_{34}, d_{34}	...	...	−12.1, ...
c_{41}, d_{41}	...	...	−12.4, ...
c_{42}, d_{42}	...	...	−21.3, ...
c_{43}, d_{43}	...	37.1, 37.1	−19.4, ...
c_{44}, d_{44}	...	...	−9.32, ...
c_{53}, d_{53}	...	7.70, 7.90	...
c'_{11}, d'_{11}	...	...	57.6, ...
c'_{12}, d'_{12}	...	...	−101.2, ...
c'_{13}, d'_{13}	...	...	−29.6, ...
c'_{14}, d'_{14}	...	...	−48.5, ...
c'_{15}, d'_{15}	...	...	−19.3, ...
c'_{16}, d'_{16}	...	...	−13.1, ...
c'_{21}, d'_{21}	...	...	92.9, ...
c'_{22}, d'_{22}	...	...	−46.1, ...
c'_{23}, d'_{23}	...	...	−34.1, ...
c'_{24}, d'_{24}	...	...	−36.5, ...
c'_{25}, d'_{25}	...	...	−33.0, ...
c'_{26}, d'_{26}	...	...	−5.90, ...
c'_{31}, d'_{31}	...	...	50.2, ...
c'_{32}, d'_{32}	...	...	6.29, ...
c'_{33}, d'_{33}	...	...	−20.0, ...
c'_{34}, d'_{34}	...	...	−22.2, ...
c'_{35}, d'_{35}	...	...	−18.6, ...
c'_{36}, d'_{36}	...	...	−6.85, ...
c'_{41}, d'_{41}	...	...	24.6, ...
c'_{42}, d'_{42}	...	...	9.61, ...
c'_{43}, d'_{43}	...	...	−6.81, ...
c'_{44}, d'_{44}	...	...	−12.6, ...
c'_{45}, d'_{45}	...	...	−11.2, ...
c'_{46}, d'_{46}	...	...	−7.22, ...

III. RESULTS AND DISCUSSION

The three systems with hindered rotations that are considered here have different levels of coupling, as can be seen in Tables I and II. Of the three studied systems, propane is the molecule with the weakest coupling between torsions. It presents only one minimum, **S1-M1**, but nine non-distinguishable wells, which are generated from the internal rotation about the C-C bonds, as shown in Fig. 2. Table I shows that a Fourier series with one term of the type $\cos(3\phi)$ for both torsional angles, together with two small coupling terms is enough for fitting the hindered rotor potential energy surface.

In the case of propane the STES and 2D-NS partition functions are very similar (Table III), but the weak coupling between the torsions splits the two torsional frequencies. They have a common value of 255 cm^{-1} when calculated with Eq. (35), but have values of 226 cm^{-1} and 289 cm^{-1}, respectively, when calculated with Eq. (36). The electronic-structure normal-mode frequencies confirm this splitting; the lowest torsional frequency corresponds to the motion of two methyl groups rotating in opposite directions, whereas the highest frequency is associated to the rotation in the same direction.

Methyl formate presents two distinguishable minima, a *cis* form, **S2-M1**, which is about 2000 cm^{-1} more stable than the *trans* form. Without doing a global fit to the two-dimensional potential energy surface, an approximate way of looking at the coupling is to scan one of the dihedral angles, but optimizing the other dihedral to its equilibrium value. If the equilibrium value remains constant with the variation of the other angle, then there is no coupling between the two torsions. When proceeding this way for both torsions, the two one-dimensional potentials are obtained. These potentials are used to calculate the STES partition functions; however, as mentioned in Sec. II, they are different from the one-dimensional potentials of Eq. (10), which are obtained from the fit by Fourier series to the two-dimensional potential energy surface.

For methyl formate the coupling is somewhat stronger than for propane, as shown in Fig. 2, which plots the slight dependence of ϕ_1 on ϕ_2. In the *cis* structure, the three hydrogen atoms of the methyl group form dihedral angles of 60°, 180°, and 300°, respectively, with respect to the molecular chain, but in the *trans* structure those dihedrals are of 0°, 120°, and 240°, respectively. Thus, the methyl group also rotates during the scan about the ϕ_1 torsional angle (Fig. 2). In the initial *cis* structure ($\phi_1 = 0°$) one of the hydrogen atoms of the methyl group has a dihedral angle of $\phi_2 = 60°$, whereas in the final *cis* structure ($\phi_1 = 360°$) the dihedral is $\phi_2 = 180°$. Both initial and final structures are the same because the hydrogen atoms within the methyl group are indistinguishable, but this

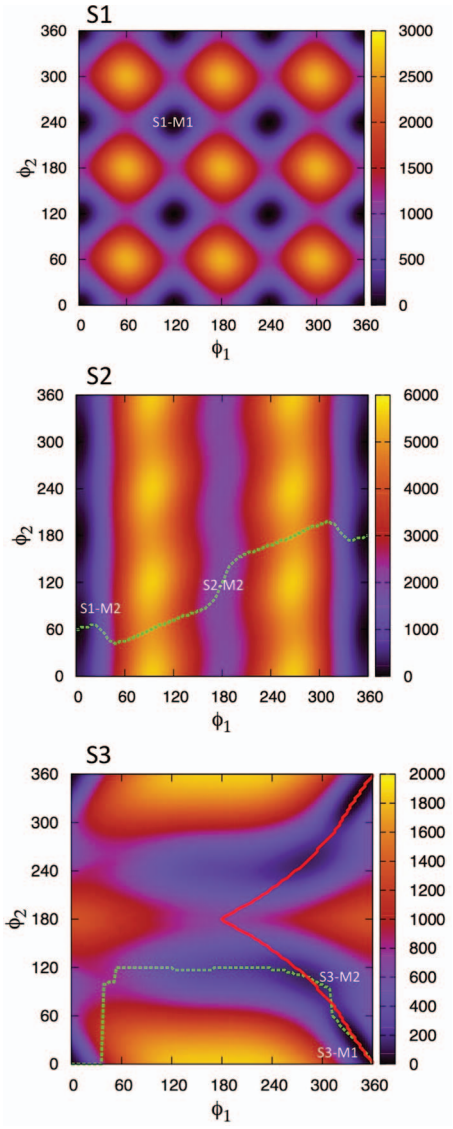

FIG. 2. Colour contour plot of the energy landscape (in cm^{-1}) resulting from the rotation about the two torsional angles. The solid-red and dashed-green lines when displayed, indicate the one-dimensional torsional potentials.

variation of ϕ_2 with ϕ_1 shows that there is coupling between the two torsions.

The HCO group is highly asymmetric and there is an important change in the partition function due of the variation of the reduced moments of inertia associated to ϕ_1 (Table IV). Thus, at $T = 100$ K there is a 25% difference between the 2D-NS partition function and the partition function ($Q^{\text{NS–V}}$ in Table III) obtained considering a Hamiltonian with coupling just in the potential energy, i.e.,

$$H^{\text{NS–V}} = \frac{-\hbar^2}{2}\left\{\frac{1}{I_1}\frac{\partial^2}{\partial\phi_1^2} + \frac{1}{I_2}\frac{\partial^2}{\partial\phi_2^2}\right\} + V_{\text{tor}}(\phi_1, \phi_2). \quad (53)$$

The difference between $Q^{\text{2D–NS}}$ and $Q^{\text{NS–V}}$ decreases with temperature, but at $T = 300$ K is still above 10%. These results indicate that coupling in the kinetic energy should be taken into account for hindered rotations about asymmetric groups. An approximated way of dealing with the coupling in the kinetic energy using just the $Q^{\text{NS–V}}$ quantum partition function would be to multiply this function by the ratio between the classical partition function given by Eq. (30) and the classical partition function obtained using constant uncoupled reduced moments of inertia. At $T = 300$ K, the partition function calculated in this approximate manner is 1.08, which is in very good agreement with 1.07 (the value obtained using the 2D-NS partition function).

TABLE III. Partition functions for the three systems calculated at several temperatures. $Q_{\text{cl, tor}}$, Q^{STES}, and $Q^{\text{2D–NS}}$ are given by Eq. (30), Eq. (20), and Eq. (28), respectively. $Q^{\text{NS–V}}$ is calculated the same way as $Q^{\text{2D–NS}}$, but considering that the reduced moments of inertia are constant and calculated at the equilibrium geometries of the the absolute minima.

System	T(K)	$Q_{\text{cl, tor}}$	Q^{STES}	$Q^{\text{NS–V}}$	$Q^{\text{2D–NS}}$
S1	100	0.0760	0.0270	0.0297	0.0288
	200	0.314	0.241	0.249	0.245
	300	0.735	0.668	0.670	0.663
	500	2.22	2.22	2.17	2.15
	700	4.61	4.77	4.59	4.55
	1000	9.78	10.2	9.78	9.70
	2000	34.9	36.6	35.2	34.9
S2	100	0.1113	0.0534	0.0578	0.0460
	200	0.506	0.438	0.465	0.403
	300	1.18	1.16	1.21	1.07
	500	3.25	3.39	3.52	3.16
	700	6.26	6.51	6.82	6.18
	1000	12.8	13.2	13.8	12.8
	2000	55.8	55.1	56.4	55.8
S3	100	1.08	1.68	0.596	0.580
	200	6.53	11.9	5.93	5.80
	300	17.6	31.7	17.4	16.9
	500	56.0	93.3	57.5	55.4
	700	112	174	117	112
	1000	219	316	230	219
	2000	677	862	717	677

The system **S3** presents two transition states **S3-M1** and **S3-M2**, both of them having enantiomers. These transition states have also been reported by Zhou *et al.*[49] when studying the hydrogen abstraction reactions from propanone by the OH radical. However, those authors considered that **S3-M1** and **S3-M2** belong to different paths for reaction, but both configurations and their enantiomers can be reached by rotation about the two torsional angles, and therefore can be treated using the same two-dimensional hindered rotor potential energy surface. For **S3** there is a third torsion about the unreacting methyl group, but it is reasonable to assume that this rotor is weakly coupled to the rest of degrees of freedom, and therefore the STES method would accurately described this motion. Hereafter, I focus on the two torsions depicted in Fig. 1. As shown in Fig. 2, there is a strong coupling between both torsions, because the one-dimensional potentials of one of the torsions involve substantial changes in the other torsion. The ratio of $Q^{\text{2D–NS}}/Q^{\text{STES}}$ (Fig. 3), which is a measure of the strength of the coupling between the torsions, is quite close to the unity for both propane and methyl formate (the parameters for the one-dimensional potentials and the graphs with the fitting for the three systems are given in the supplementary material.[32]). However, for system **S3** there is a substantial deviation from the unity. This is expected, because the STES

TABLE IV. Some parameters of interest for the two internal rotations of the three systems. The minima **S3-M1** and **S3-M2** have enantiomers. The frequencies $\omega_{i,1}$ and $\omega_{i,2}$ correspond to normal-mode torsional frequencies, whereas $\overline{\omega}^{\star}_{i,1}$, $\overline{\omega}^{\star}_{i,2}$, and $\overline{\omega}_{i,1}$ and $\overline{\omega}_{i,2}$ are the frequencies calculated by Eqs. (35) and (36), respectively. The zero-point energies (ZPE) calculated by the STES and 2D-NS methods are also indicated. All the frequencies, ZPEs, and the energy difference between conformers U_i are given in cm^{-1}. The reduced moments of inertia are given in amu $Å^2$.

System	Wells	σ_1, σ_2	Conformer	$\omega_{i,1}, \omega_{i,2}$	$\overline{\omega}^{\star}_{i,1}, \overline{\omega}^{\star}_{i,2}$	$\overline{\omega}_{i,1}, \overline{\omega}_{i,2}$	ZPE^{STES}	ZPE^{2D-NS}	I_1, I_2	U_i
S1	9	3, 3	**S1-M1**	219, 270	255, 255	226, 289	256	251	2.667, 2.667	0
S2	6	1, 3	**S2-M1**	310, 130	310, 128	344, 128	221	232	3.531, 2.954	0
			S2-M2	187, 58	192, 63	195, 34			5.761, 2.331	2015
S3	4	1, 1	**S3-M1**	421, 34	409, 67	412, 42	114	207	0.884, 24.91	0
			S3-M2	158, 42	151, 48	152, 40			0.867, 25,91	119

method is based on two one-dimensional potentials that have torsional frequencies substantially different from the ones of the two-dimensional potential. Thus, the zero-point energy due to the two torsions calculated with STES is 114 cm^{-1}, whereas the one calculated with 2D-NS is 207 cm^{-1}, and thus Q^{STES} increases much faster. Actually, the coupling is also important at high temperatures, and the ratio Q^{2D-NS}/Q^{STES} never converges to the unity (it has a limiting value of 0.80). This example shows that when the coupling is strong, the one-dimensional potentials are not able to reproduce all the features of the bi-dimensional potential and the STES approximation fails.

The MC-PG partition function, which in principle is less accurate than STES, gives better results when compared to 2D-NS, and the ratios F_q/F^{MC-PG} are all very close to the unity (Fig. 4). This is a remarkable result taking into account that the F^{MC-PG} coefficient is based on the HO approximation. These examples indicate that MC-PG could be an approximate, but less expensive, alternative to 2D-NS. One important issue is that for the evaluation of Q^{MC-PG} we need to know the torsional frequencies. As shown in Table IV, the differences between $\overline{\omega}^{\star}_{\tau}$ and $\overline{\omega}_{\tau}$ in some cases (for instance, **S1-M1**, **S2-M1**, and **S3-M1**), reveals the importance of taking into account the off-diagonal terms in the calculation of the torsional frequencies. Actually, these three systems indicate that if the calculation of the $\overline{\omega}_{\tau}$ frequencies is difficult, it would be better to use the normal-mode frequencies than the $\overline{\omega}^{\star}_{\tau}$ frequencies in the evaluation of Q^{MC-PG}.

Finally, to show the adequacy of the multi-dimensional partition function of Eq. (50), the standard state entropies S^o and heat capacities at constant pressure C_p^o at $T = 298.15$ K for reactions **S1** and **S2** have been calculated. For system **S1**, the values using Eq. (50) are $S^o = 64.73$ cal K^{-1} mol^{-1} and $C_p^o = 17.59$ cal K^{-1} mol^{-1} that compare very well with the experimental values of $S^o = 64.6$ cal K^{-1} mol^{-1} and $C_p^o = 17.6$ cal K^{-1} mol^{-1}.[50] The results are also good for methyl formate for which the calculated values are $S^o = 68.32$ cal K^{-1} mol^{-1} and $C_p^o = 15.14$ cal K^{-1} mol^{-1}, whereas the experimental values are $S^o = 68.18$ cal K^{-1} mol^{-1} and $C_p^o = 15.40$ cal K^{-1} mol^{-1}.[51] These results are encouraging, and the application to chemical reactions of the 2D-NS methodology described in this work, together with Eq. (50) is on its way.

In this context, Eq. (50) can be easily implemented within the framework of variational transition state theory,[52] and it is expected that the 2D-NS method would lead to an important improvement over the harmonic approximation in the calculation of thermal rate constants and kinetic isotope effects of chemical reactions with two strongly coupled hindered rotations.

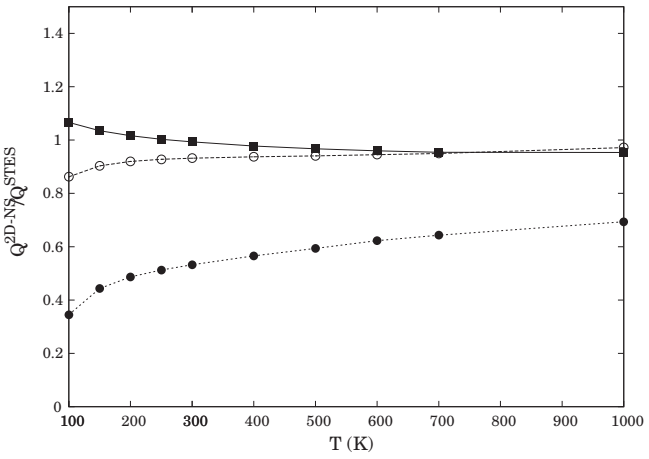

FIG. 3. Plot of the ratio Q^{2D-NS}/Q^{STES} at several temperatures. The ratios for systems **S1**, **S2**, and **S3** are represented by filled squares, circles, and filled circles, respectively.

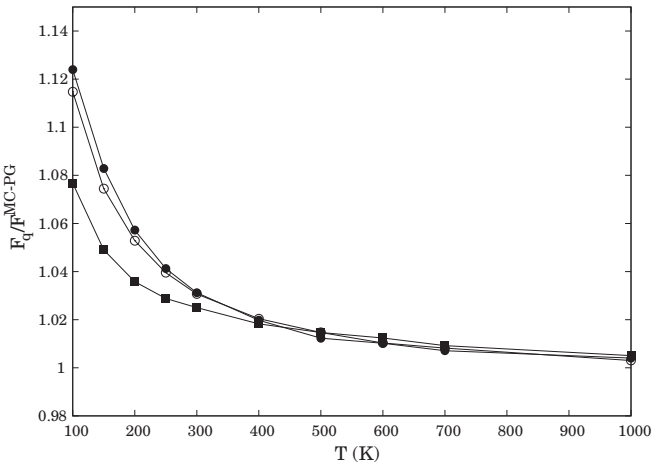

FIG. 4. Plot of the ratio F_q/F^{MC-PG} at several temperatures. Symbols as for Fig. 3.

ACKNOWLEDGMENTS

This work was partially financed by Xunta de Galicia through Grant No. 2012/314 para a consolidación e a estruturación de unidades de investigación competitivas do Sistema Universitario de Galicia, 2012. The author thanks Dr. Rubén Meana-Pañeda for helpful discussions.

[1] K. S. Pitzer, J. Chem. Phys. **5**, 469 (1937).
[2] K. S. Pitzer and W. D. Gwinn, J. Chem. Phys. **10**, 428 (1942).
[3] D. G. Truhlar, J. Comput. Chem. **12**, 266 (1991).
[4] R. B. McClurg, R. C. Flagan, and W. A. Goddard III, J. Chem. Phys. **106**, 6675 (1997); **111**, 7165 (1999) (Erratum).
[5] P. Y. Ayala and H. B. Schlegel, J. Chem. Phys. **108**, 2314 (1998).
[6] Y. Y. Chuang and D. G. Truhlar, J. Chem. Phys. **112**, 1221 (2000); **121**, 7036 (2004) (Erratum); **124**, 179903 (2006) (Erratum).
[7] B. A. Ellingson, V. A. Lynch, S. L. Mielke, and D. G. Truhlar, J. Chem. Phys. **125**, 084305 (2006).
[8] C. Y. Lin, E. I. Izgorodina, and M. L. Coote, J. Phys. Chem. A **112**, 1956 (2008).
[9] M. L. Strekalov, Chem. Phys. **362**, 75 (2009).
[10] V. Van Speybroeck, P. Vansteenkiste, D. Van Neck, and M. Waroquier, Chem. Phys. Lett. **402**, 479 (2005).
[11] S. L. Mielke and D. G. Truhlar, J. Chem. Phys. **114**, 621 (2001).
[12] S. L. Mielke and D. G. Truhlar, J. Chem. Phys. **115**, 652 (2001).
[13] T. F. Miller and D. C. Clary, J. Chem. Phys. **116**, 8262 (2002).
[14] T. F. Miller and D. C. Clary, Mol. Phys. **103**, 1573 (2005).
[15] Y. K. Sturdy and D. C. Clary, Phys. Chem. Chem. Phys. **9**, 2065 (2007).
[16] Y. K. Sturdy and D. C. Clary, Phys. Chem. Chem. Phys. **9**, 2397 (2007).
[17] J. Janakiraman and K. L. Sebastian, Comput. Theor. Chem. **988**, 6 (2012).
[18] M. L. Edinoff and J. G. Aston, J. Chem. Phys. **3**, 379 (1935).
[19] M. Tafipolsky and R. Schmid, J. Comput. Chem. **26**, 1579 (2005).
[20] S. Sharma, S. Raman, and W. H. Green, J. Phys. Chem. A **114**, 5689 (2010).
[21] J. Zheng, T. Yu, E. Papajak, I. M. Alecu, S. L. Mielke, and D. G. Truhlar, Phys. Chem. Chem. Phys. **13**, 10885 (2011).
[22] T. Yu, J. Zheng, and D. G. Truhlar, Chem. Sci. **2**, 2199 (2011).
[23] P. Vansteenkiste, V. Van Speybroeck, E. Pauwels, and M. Warroquier, Chem. Phys. **314**, 109 (2005).
[24] P. Vansteenkiste, T. Verstraelen, V. Van Speybroeck, and M. Warroquier, Chem. Phys. **328**, 251 (2006).
[25] P. Groner and J. R. Durig, J. Chem. Phys. **66**, 1856 (1977).
[26] J. R. Durig, M. G. Griffin, and P. Groner, J. Phys. Chem. **81**, 554 (1977).
[27] M. L. Senent, M. Villa, F. J. Meléndez, and R. Domínguez-Gómez, Astrophys. J. **627**, 567 (2005).
[28] E. Darian, V. Hnizdo, A. Fedorowicz, H. Singh, and E. Demchuk, J. Comput. Chem. **26**, 651 (2005).
[29] A. L. L. East and L. Radom, J. Chem. Phys. **106**, 6655 (1997).
[30] J. E. Kilpatrick and K. S. Pitzer, J. Chem. Phys. **17**, 1064 (1949).
[31] K. S. Pitzer, J. Chem. Phys. **14**, 239 (1946).
[32] See supplementary material at http://dx.doi.org/10.1063/1.4798407 for the integrals to obtain the matrix elements of Eq. (16); the matrix elements that include the derivative of $d_{\tau\zeta}$ in Eq. (26); the geometries and frequencies of the stationary points depicted in Fig. 1; the parameters used to fit the Fourier series of the $d_{\tau\zeta}$ elements of the kinetic energy; and the parameters and plots for the one-dimensional potentials.
[33] J. Pfaendtner, X. Yu, and L. J. Broadbelt, Theor. Chem. Acc. **118**, 881 (2007).
[34] J. R. Durig, P. Groner, and M. G. Griffin, J. Chem. Phys. **66**, 3061 (1977).
[35] Y. G. Smeyers and M. N. Bellido, Int. J. Quantum Chem. **19**, 553 (1981).
[36] Y. G. Smeyers and M. N. Bellido, Int. J. Quantum Chem. **23**, 507 (1983).
[37] A. Fernández-Ramos, B. A. Ellingson, R. Meana-Pañeda, J. M. C. Marques, and D. G. Truhlar, Theor. Chem. Acc. **118**, 813 (2007).
[38] P. Vansteenkiste, D. Van Neck, V. Van Speybroeck, and M. Waroquier, J. Chem. Phys. **124**, 044314 (2006); **125**, 049902 (2006) (Erratum).
[39] R. Meana-Pañeda and A. Fernández-Ramos, J. Am. Chem. Soc. **134**, 346 (2012); **134**, 7193 (2012) (Erratum).
[40] Y. Zhao, B. J. Lynch, and D. G. Truhlar, J. Phys. Chem A **108**, 6908 (2004).
[41] W. J. Hehre, R. Ditchfield, and J. A. Pople, J. Chem. Phys **56**, 2257 (1972).
[42] Y. Zhao, N. E. Schultz, and D. G. Truhlar, J. Chem. Theory Comput. **2**, 364 (2006).
[43] J. Zheng, S. L. Mielke, K. L. Clarkson, and D. G. Truhlar, Comput. Phys. Commun. **183**, 1803 (2012).
[44] I. M. Alecu, J. Zheng, Y. Zhao, and D. G. Truhlar, J. Chem. Theory Comput. **6**, 2872 (2010).
[45] R. J. Renka, ACM Trans. Math. Softw. **19**, 81 (1993).
[46] GNUplot version 4.2, 2012; see http://www.gnuplot.info.
[47] M. Bollhöfer and Y. Notay, Comput. Phys. Commun. **177**, 951 (2007).
[48] A. Fernández-Ramos, "HR2D version 1.0, Universidade de Santiago de Compostela, Santiago de Compostela" (2012).
[49] C.-W. Zhou, J. M. Simmie, and H. J. Curran, Phys. Chem. Chem. Phys. **13**, 11175 (2011).
[50] J. Chao, R. C. Wilhoit, and B. J. Zwolinski, J. Phys. Chem. Ref. Data **2**, 427 (1973).
[51] J. Chao, K. R. Hall, K. N. Marsch, and R. C. Wilhoit, J. Phys. Chem. Ref. Data **15**, 1369 (1986).
[52] A. Fernández-Ramos, A. Ellingson, B. C. Garrett, and D. G. Truhlar, Rev. Comput. Chem. **23**, 125 (2007).